A Marginalized Likelihood Ratio Approach for detecting and estimating multipath biases on GNSS measurements

Cheng Cheng, Jean-Yves Tourneret, Quan Pan, Vincent Calmettes

A Marginalized Likelihood Ratio Approach for Detecting and Estimating Multipath Biases on GNSS Measurements

Cheng CHENG [1, 2], Jean-Yves TOURNERET [3], Quan PAN [1], Vincent CALMETTES [2]
1. School of Automation, Northwestern Polytechnical University
Key Laboratory of Information Fusion Technology, Ministry of Education of China, Xi'an, China
Email: cheng.cheng418@gmail.com, quanpan@nwpu.edu.cn
2. ISAE-Supaéro, University of Toulouse, Toulouse, France
Email: cheng.cheng@isae.fr, vincent.calmettes@isae.fr
3. ENSEEIHT-IRIT, University of Toulouse, Toulouse, France
Email: jean-yves.tourneret@enseeiht.fr

Abstract: **In urban canyons, non-line-of-sight (NLOS) multipath interferences affect position estimation based on Global Navigation Satellite Systems (GNSS). In this paper, the effects of NLOS multipath interferences are modeled as mean value jumps appearing on the GNSS pseudo-range measurements. The Marginalized Likelihood Ratio Test (MLRT) is proposed to detect, identify and estimate the NLOS multipath biases. However, the MLRT test statistics is generally difficult to compute. In this work, we consider a Monte Carlo integration technique based on bias magnitude sampling. The Jensen inequality allows this Monte Carlo integration to be simplified. The interacting multiple model algorithm is also used to update the prior information for each bias magnitude sample. Finally, some strategies are designed for estimating and correcting the NLOS multipath biases. Simulation results show that the proposed approach can effectively improve the positioning accuracy in the presence of NLOS multipath interferences.**

***Keywords**: GNSS; multipath mitigation; MLRT; multiple model; urban positioning.*

I. INTRODUCTION

Global Navigation Satellite Systems (GNSS) are widely applied for the surveillance of mini unmanned aerial /landing vehicles or the search and rescue in urban canyon scenarios. In these applications, multipath (MP) interference is one of the largest sources of GNSS errors. MP errors are due to the fact that a signal emitted from a satellite is very likely to get reflected and to follow different paths before arriving to the GNSS receiver [1]. MP interferences can be divided into two classes: (a) the line-of-sight (LOS) interferences which result from the signal composed of the sum of the direct signal and of delayed reflections; (b) the non-line-of-sight (NLOS) interferences which result from a unique reflected signal received and tracked by the GNSS receiver [2]. In urban canyons, the direct path of the satellite signal is vulnerable to masking or blocking and the GNSS receiver is likely to track reflected signals. Therefore, NLOS MP interferences frequently happen in urban canyons.

Different approaches can be found in the literature for mitigating MP interference errors. First, the use of high quality antennas or antenna arrays has shown to be efficient for detecting GNSS measurements affected by MP interferences and exclude them from the positioning operation [2], [3]. Unfortunately, these antennas are expensive and have large dimensions. Second, considering that the GNSS receiver has to track the signal composed of the direct signal and of delayed reflections in the LOS situation, several MP mitigation methods based on the Delay Lock Loop (DLL) tracking have been proposed. These methods include the MP insensitive delay lock loop [4], the multicorrelator GNSS receivers [5] and the adaptive vector-tracking loop [6] et al.. In the NLOS situation, the MP interferences can be hardly mitigated by these strategies while the direct signal is blocked or masked. To overcome these difficulties, one can compare visible satellites with a priori knowledge of the shadowed satellites [7]. Another possibility is to exploit the geometric path model [8] or a 3D model of the environment [9] in order to estimate a possible reflection path of NLOS MP interferences. The reflected signal due to a MP interference can be converted to a bias appearing on the GNSS pseudo-range measurement. When prior information for this bias can be obtained [10], MP mitigation methods based on Bayesian statistical theory for GNSS pseudo-range measurements can be considered. For instance, Spangenberg considered in [11] two different models for pseudo-range measurements depending on the availability of LOS signals. Viandier proposed in [12] different ways of handling pseudo-range measurements contaminated by MP biases in urban scenarios, and of estimating the position of a vehicle by using a particle filter applied to a jump Markov system. Giremus proposed in [13] a fixed Rao-Blackwellized particle filter to jointly detect and estimate MP biases associated with GNSS pseudo-range measurements.

Some bias detection methods are based on the Generalized Likelihood Ratio Test (GLRT) and the Marginalized Likelihood Ratio Test (MLRT) [14], [15]. However, the

marginal likelihood function of the MLRT is generally difficult to compute. This problem has been addressed in [16] where a numerical solution based on the unscented transform was proposed. Accordingly, this paper proposes an approximate MLRT to detect, identify and estimate the NLOS MP biases affecting GNSS pseudo-range measurements.

The paper is organized as follows: The system considered for GNSS positioning is introduced in Section II. Section III studies the MLRT and its approximation based on Jensen's Inequality to detect MP biases in GNSS measurements. Section IV investigates the identification, estimation and correction of GNSS measurement in the presence of NLOS MP biases. Simulation results and conclusions are reported in Sections V and VI respectively.

II. SYSTEM DESCRIPTION

A. State Model

We consider a second-order model (i.e., constant velocity model) to describe the dynamic of the vehicle in the Earth Centered Earth Fixed (ECEF) frame. Moreover, the GNSS receiver clock offset and its drift are taken into account. Therefore, the state model can be divided into two parts containing the position and velocity of the vehicle in the ECEF frame, and the receiver clock offset and drift, respectively. More precisely, the state vector considered in this paper is defined as follows [1]

$$\boldsymbol{X}_t = (x_t, \dot{x}_t, y_t, \dot{y}_t, z_t, \dot{z}_t, b_t, d_t)^T,$$

where

- (x_t, y_t, z_t) is the vehicle position in the ECEF frame,
- $(\dot{x}_t, \dot{y}_t, \dot{z}_t)$ is the vehicle velocity,
- b_t and d_t are the GNSS receiver clock offset and its drift respectively.

The velocity can be reasonably modeled as a random walk process, e.g., $\ddot{x}_t = \omega_x$ where ω_x is a zero mean Gaussian noise of variance σ_a^2. For short-term applications in which the periodical clock resets of the GNSS receiver are not taken into account, the GNSS receiver clock offset b_t and its drift d_t can also be modeled as random walk processes, i.e., $\dot{b}_t = d_t + \omega_b$ and $\dot{d}_t = \omega_d$ where ω_b and ω_d are zero-mean Gaussian white noises of variance σ_b^2 and σ_d^2. Based on the above assumptions, the discrete-time state model which describes the propagation of the vehicle state $\boldsymbol{X}_t$ can be formulated as

$$\boldsymbol{X}_{k+1} = \boldsymbol{\Phi}_{k+1/k}\boldsymbol{X}_k + \boldsymbol{\omega}_k, \tag{1}$$

where

- $k = 1, \dots, \infty$ denotes the sampling time instants.
- $\boldsymbol{\omega}_k = (\omega_x, \omega_y, \omega_z, \omega_b, \omega_d)^T$ is the zero mean Gaussian white noise vector of covariance matrix $\boldsymbol{Q}_k$.

Considering a relative independence between the kinematic parameters and the GNSS clock parameters, the state matrix $\boldsymbol{\Phi}_{k+1/k}$ is a block-diagonal matrix. The matrices $\boldsymbol{\Phi}_{k+1/k}$ and $\boldsymbol{Q}_k$ can be defined as follows

$$\boldsymbol{\Phi}_{k+1/k} = \begin{pmatrix} \boldsymbol{A}_k & \boldsymbol{0} \\ \boldsymbol{0} & \boldsymbol{C}_k \end{pmatrix} \text{ and } \boldsymbol{Q}_k = \begin{pmatrix} \boldsymbol{\Sigma}_k^a & \boldsymbol{0} \\ \boldsymbol{0} & \boldsymbol{\Sigma}_k^c \end{pmatrix},$$

where the block matrices $\boldsymbol{A}_k$, $\boldsymbol{C}_k$, $\boldsymbol{\Sigma}_k^a$ and $\boldsymbol{\Sigma}_k^c$ are precised below

$$\boldsymbol{A}_k = \begin{pmatrix} \boldsymbol{C}_k & \boldsymbol{0} & \boldsymbol{0} \\ \boldsymbol{0} & \boldsymbol{C}_k & \boldsymbol{0} \\ \boldsymbol{0} & \boldsymbol{0} & \boldsymbol{C}_k \end{pmatrix} \text{ with } \boldsymbol{C}_k = \begin{pmatrix} 1 & \Delta t \\ 0 & 1 \end{pmatrix},$$

$$\boldsymbol{\Sigma}_k^a = \begin{pmatrix} \boldsymbol{Q}_k^a & \boldsymbol{0} & \boldsymbol{0} \\ \boldsymbol{0} & \boldsymbol{Q}_k^a & \boldsymbol{0} \\ \boldsymbol{0} & \boldsymbol{0} & \boldsymbol{Q}_k^a \end{pmatrix} \text{ with } \boldsymbol{Q}_k^a = \begin{pmatrix} \sigma_a^2 \frac{\Delta t^4}{4} & \sigma_a^2 \frac{\Delta t^3}{2} \\ \sigma_a^2 \frac{\Delta t^3}{2} & \sigma_a^2 \Delta t^2 \end{pmatrix},$$

$$\boldsymbol{\Sigma}_k^c = \begin{pmatrix} \sigma_b^2 \Delta t^2 + \sigma_d^2 \frac{\Delta t^4}{4} & \sigma_d^2 \frac{\Delta t^3}{2} \\ \sigma_d^2 \frac{\Delta t^3}{2} & \sigma_d^2 \Delta t^2 \end{pmatrix},$$

and where Δt represents the time interval between two successive sampling time instants.

B. Measurement Model

Assuming that the MP bias drift is very slow for the considered vehicle, we introduce a mean value jump affecting the GNSS pseudo-range measurements in the presence of NLOS MP interferences. Consequently, the τ-th in-view satellite pseudo-range measurement model including an NLOS MP bias can be defined as

$$Z_k^\tau = \sqrt{(x_k^\tau - x_k)^2 + (y_k^\tau - y_k)^2 + (z_k^\tau - z_k)^2} + b_k + v_{k,\theta}^\tau + \omega_k^r, \tag{2}$$

where

- Z_k^τ $(\tau = 1, \dots, N_s)$ is the pseudo-range measurement associated with the τ-th in-view satellite, and N_s is the number of in-view satellites,
- $(x_k^\tau, y_k^\tau, z_k^\tau)$ and (x_k, y_k, z_k) are the τ-th satellite position and the vehicle position in the ECEF frame respectively,
- b_k is the GNSS receiver clock offset,
- $v_{k,\theta}^\tau$ is the magnitude of the NLOS MP bias associated with the τ-th pseudo-range measurement, θ represents the possible occurrence time of the NLOS MP bias, and $\theta = k$ for $v = 0$,
- ω_k^r is the τ-th satellite pseudo-range measurement noise with $\omega_k^r \sim \mathcal{N}(0, \sigma_r^2)$, and $\mathcal{N}(\cdot)$ represents the Gaussian distribution.

In (2), the pseudo-range measurement related to the vehicle position is defined by a non-linear equation. The unscented Kalman filter (UKF) and the particle filter (PF) could be investigated to estimate the state of this nonlinear estimation problem. However, the corresponding computational costs can be prohibitive for practical applications. Thus, we consider in this paper an extended Kalman filter (EKF) which linearizes the non-linear equations (2) and provides an efficient and low-cost solution for weakly nonlinear systems.

III. NLOS BIAS DETECTION BASED ON MLRT

A. Problem Formulation

In the NLOS situation, we propose to model the MP interference as a mean value jump affecting the GNSS pseudo-range measurements. According to the hypothesis testing theory, the likelihood ratio test (LRT) for detecting the

presence of a mean value jump is a binary hypothesis test which compares two hypotheses associated with the absence (H_0) and presence (H_1) of a mean value jump in the measurements. The two hypotheses considered in this paper are defined as follows

H_0: no mean value jump up to present time k

H_1: a mean value jump (of amplitude $v \neq 0$) has occurred at time $\theta < k$

The log-likelihood ratio (LLR) for these two hypotheses is

$$l_k(\theta, v) = 2 \ln \frac{p\left(\boldsymbol{Z}_{1:k} \middle| \mathrm{H}_1(\theta, v)\right)}{p(\boldsymbol{Z}_{1:k} | \mathrm{H}_0)}, \quad (3)$$

where $\boldsymbol{Z}_{1:k} = \{\boldsymbol{Z}_i\}_{i=1}^{k}$ and $\boldsymbol{Z}_i = \left(Z_i^1, \ldots, Z_i^{N_s}\right)$ is the pseudo-range measurement vector sequence up to time k, and N_s is the number of in-view satellites. Denote as $p\left(\boldsymbol{Z}_{1:k} \middle| \mathrm{H}_1(\theta, v)\right)$ and $p(\boldsymbol{Z}_{1:k} | \mathrm{H}_0)$ the probability density functions (pdfs) of the measurement vector associated with the hypotheses H_0 and H_1 respectively.

In the likelihood ratio test, the occurrence time and magnitude of the mean value jump denoted as θ and v are assumed to be known. However, the unknown jump magnitude v can be regarded as a nuisance parameter for the LRT. According to the literature, there are two classes of methods for eliminating the nuisance parameter v. The first method consists of replacing the nuisance parameter by its maximum likelihood estimator (MLE) (maximizing the likelihood function) in the pdf $p\left(\boldsymbol{Z}_{1:k} \middle| \mathrm{H}_1(\theta, v)\right)$ leading to the Generalized Likelihood Ratio Test (GLRT). The second method marginalizes the LLR with respect to the nuisance parameter yielding the Marginalized Likelihood Ratio Test (MLRT). The key point of the GLRT based on a state space model is that the MLE of parameter v can be obtained by the innovation from a Kalman filter. Contrary to the GLRT, the nuisance parameter v is eliminated by marginalization of the likelihood function under the hypothesis H_1 in the MLRT. In [15], Gustafsson proposed an MLRT approach based on a space state model as an alternative more robust method for bias detection. Unfortunately, the marginal likelihood function under hypothesis H_1 is generally difficult to compute. An alternative was proposed by Giremus in [16] where a numerical solution of MLRT based on the unscented transform was used for bias detection in space state models. The method studied in [16] introduced a prior distribution for the nuisance parameter v which can be obtained from our experience about MP or from previous experiments. This paper studies a similar approach which differs from [16] by the use of an approximation based on Jensen's inequality, as explained below. According to the error envelope of MP interferences which is a function of the MP relative delay interfering the direct signal for a given GNSS receiver configuration [10], a suitable prior distribution for the MP bias with magnitude v is a uniform distribution defined by,

$$p(v) \sim \mathrm{U}(v_{min}, v_{max}),$$

where

- $\mathrm{U}(\cdot)$ represents the uniform distribution,
- v_{min} and v_{max} are the maximum and minimum magnitudes of the MP bias, respectively.

Using this prior distribution for the nuisance parameter, we propose in this paper an approximate MLRT based on Jensen's inequality to detect the occurrence time of NLOS MP biases.

The marginalization of (3) with respect to v leads to

$$l_k(\theta) = 2 \ln \frac{p\left(\boldsymbol{Z}_{1:k} \middle| \mathrm{H}_1(\theta)\right)}{p(\boldsymbol{Z}_{1:k} | \mathrm{H}_0)}, \quad (4)$$

where

$$p\left(\boldsymbol{Z}_{1:k} \middle| \mathrm{H}_1(\theta)\right) = \int p\left(\boldsymbol{Z}_{1:k} \middle| \mathrm{H}_1(\theta, v)\right) p(v)\, dv, \quad (5)$$

and where $p(v)$ is the prior distribution of v. Considering that the integral of (5) is difficult to compute in closed-form, a Monte Carlo (MC) integration method can be used to evaluate (5). According to the MC integration, (5) is approximated as

$$p\left(\boldsymbol{Z}_{1:k} \middle| \mathrm{H}_1(\theta)\right) \approx \sum_{i=1}^{n} \omega^i p\left(\boldsymbol{Z}_{1:k} \middle| \mathrm{H}_1(\theta, v_i)\right), \quad (6)$$

where v_i $(i = 1,2, \ldots, n)$ is the i-th sampling value of the MP bias magnitude belonging to the interval (v_{min}, v_{max}), and n is the number of magnitude samples. Thus $\omega^i = 1/n$ is the corresponding weight with

$$\sum_{i=1}^{n} \omega^i = 1.$$

As a consequence, the test statistic $l_k(\theta)$ in MLRT can be approximated as

$$l_k(\theta) = 2 \ln \frac{p\left(\boldsymbol{Z}_{1:k} \middle| \mathrm{H}_1(\theta)\right)}{p(\boldsymbol{Z}_{1:k} | \mathrm{H}_0)} \approx 2 \ln \frac{\sum_{i=1}^{n} \omega^i p\left(\boldsymbol{Z}_{1:k} \middle| \mathrm{H}_1(\theta, v_i)\right)}{p(\boldsymbol{Z}_{1:k} | \mathrm{H}_0)}.$$

Since $v = 0$ for $k < \theta$, $l_k(\theta)$ can be rewritten with the following more compact expression

$$l_k(\theta) = 2 \ln \frac{\sum_{i=1}^{n} \omega^i p\left(\boldsymbol{Z}_{\theta:k} \middle| \boldsymbol{Z}_{1:\theta-1}, \mathrm{H}_1(\theta, v_i)\right)}{p(\boldsymbol{Z}_{\theta:k} | \boldsymbol{Z}_{1:\theta-1}, \mathrm{H}_0)}. \quad (7)$$

The MLE of the occurrence time θ is

$$\hat{\theta} = \underset{\theta}{\operatorname{argmax}}\, l_k(\theta).$$

According to the Neyman-Pearson lemma, the presence of a mean value jump is decided using the following MLRT rule

$$l_k(\hat{\theta}) \underset{\mathrm{H}_0}{\overset{\mathrm{H}_1}{\gtrless}} \varepsilon,$$

where ε is a threshold related to the probability of false alarm of the test. In order to reduce the computational complexity, the optimization of θ is constrained to the last L_w units of time, i.e., $k - L_w < \theta \leq k$ at any time k, and L_w is a finite window length.

B. An Approximate MLRT Based on Jensen's Inequality

According to the Kalman filter theory, the denominator of (7) which is the likelihood function associated with the hypothesis H_0 can be defined as

$$p(\boldsymbol{Z}_{\theta:k}|\boldsymbol{Z}_{1:\theta-1},\mathrm{H}_0)=\prod_{j=\theta}^{k}p\big(\boldsymbol{Z}_j\big|\boldsymbol{Z}_{1:j-1},\mathrm{H}_0\big), \tag{8}$$

with

$$p\big(\boldsymbol{Z}_j\big|\boldsymbol{Z}_{1:j-1},\mathrm{H}_0\big)=\mathcal{N}\big(\boldsymbol{Z}_j;\,\widehat{\boldsymbol{Z}}^0_{j/j-1},\boldsymbol{S}^0_j\big)=p\big(\boldsymbol{\gamma}^0_j\big|\mathrm{H}_0\big),$$

and where

- $\boldsymbol{\gamma}^0_j=\boldsymbol{Z}_j-\widehat{\boldsymbol{Z}}^0_{j/j-1}$ and $\boldsymbol{S}^0_j$ are the filter innovation vector and covariance matrix in absence of mean value jump at time j,
- $\boldsymbol{Z}_j$ and $\widehat{\boldsymbol{Z}}^0_{j/j-1}$ are the measurement and predicted measurement vector under the hypothesis H_0 at time j.

The numerator of (7) is a weighted sum of likelihood functions associated with different mean value jump hypotheses with magnitudes v_i ($i=1,\dots,n$). Thus the likelihood function under the hypothesis of a mean value jump with magnitude sampling v_i is

$$p(\boldsymbol{Z}_{\theta:k}|\boldsymbol{Z}_{1:\theta-1},\mathrm{H}_1(\theta,v_i))=\prod_{j=\theta}^{k}p\left(\boldsymbol{Z}_j\middle|\boldsymbol{Z}_{1:j-1},\mathrm{H}_1(\theta,v_i)\right), \tag{9}$$

with

$$\begin{aligned}p\left(\boldsymbol{Z}_j\middle|\boldsymbol{Z}_{1:j-1},\mathrm{H}_1(\theta,v_i)\right)&=\mathcal{N}\big(\boldsymbol{Z}_j;\,\widehat{\boldsymbol{Z}}^i_{j/j-1},\boldsymbol{S}^i_j\big)\\&=p\left(\widetilde{\boldsymbol{\gamma}}^i_j\middle|\mathrm{H}_1(\theta,v_i)\right),\end{aligned}$$

where

- $\widetilde{\boldsymbol{\gamma}}^i_j=\boldsymbol{\gamma}^0_j-v_i$ and $\boldsymbol{S}^i_j$ are the filter innovation vector and covariance matrix in the presence of a mean value jump with magnitude v_i at time j,
- $\widehat{\boldsymbol{Z}}^i_{j/j-1}$ is the predicted measurement vector under the hypothesis H_1 of magnitudes v_i at time j.

After replacing (8) and (9) in (7), the MLRT test statistic based on MC integration can be expressed as follows

$$\begin{aligned}l_k(\theta)&=2\ln\frac{\sum_{i=1}^{n}\omega^i\prod_{j=\theta}^{k}\mathcal{N}\big(\boldsymbol{Z}_j;\,\widehat{\boldsymbol{Z}}^i_{j/j-1},\boldsymbol{S}^i_j\big)}{\prod_{j=\theta}^{k}\mathcal{N}\big(\boldsymbol{Z}_j;\,\widehat{\boldsymbol{Z}}^0_{j/j-1},\boldsymbol{S}^0_j\big)}\\&=2\ln\frac{\sum_{i=1}^{n}\omega^i\prod_{j=\theta}^{k}p\left(\widetilde{\boldsymbol{\gamma}}^i_j\middle|\mathrm{H}_1(\theta,v_i)\right)}{\prod_{j=\theta}^{k}p\big(\boldsymbol{\gamma}^0_j\big|\mathrm{H}_0\big)}.\end{aligned} \tag{10}$$

According to (10), it is clear that the multiplication of several normal pdfs in the denominator can be easily handled by the logarithm function. Conversely, the numerator of (10) is a weighted sum of normal pdfs and thus is not easily tractable after the logarithm operation. Since the natural logarithm is a concave function over its range, Jensen's inequality [17] can be advocated leading to

$$\ln\sum_{i=1}^{n}\lambda_i\,g(x_i)\geq\sum_{i=1}^{n}\lambda_i\ln g(x_i), \tag{11}$$

where $g(\cdot)$ is any functional, $\lambda_i>0$ and $\sum_{i=1}^{n}\lambda_i=1$. After computing the numerator of (10), (11) leads to

$$\ln\sum_{i=1}^{n}\omega^i\prod_{j=\theta}^{k}p\left(\widetilde{\boldsymbol{\gamma}}^i_j\middle|\mathrm{H}_1(\theta,v_i)\right)\geq\sum_{i=1}^{n}\omega^i\ln\prod_{j=\theta}^{k}p\left(\widetilde{\boldsymbol{\gamma}}^i_j\middle|\mathrm{H}_1(\theta,v_i)\right). \tag{12}$$

After replacing (12) in (10), the test statistic $l_k(\theta)$ can be rewritten as follows

$$\begin{aligned}l_k(\theta)&=2\ln\frac{\sum_{i=1}^{n}\omega^i\prod_{j=\theta}^{k}p\left(\widetilde{\boldsymbol{\gamma}}^i_j\middle|\mathrm{H}_1(\theta,v_i)\right)}{\prod_{j=\theta}^{k}p\big(\boldsymbol{\gamma}^0_j\big|\mathrm{H}_0\big)}\\&\geq 2\left(\sum_{i=1}^{n}\omega^i\ln\prod_{j=\theta}^{k}p\left(\widetilde{\boldsymbol{\gamma}}^i_j\middle|\mathrm{H}_1(\theta,v_i)\right)-\ln\prod_{j=\theta}^{k}p\big(\boldsymbol{\gamma}^0_j\big|\mathrm{H}_0\big)\right)\\&\stackrel{\text{def}}{=}\tilde{l}_k(\theta).\end{aligned} \tag{13}$$

i.e.,

$$\tilde{l}_k(\theta)=\left[\sum_{j=\theta}^{k}\big(\boldsymbol{\gamma}^0_j\big)^T\big(\boldsymbol{S}^0_j\big)^{-1}\big(\boldsymbol{\gamma}^0_j\big)-\sum_{i=1}^{n}\omega^i\sum_{j=\theta}^{k}\big(\widetilde{\boldsymbol{\gamma}}^i_j\big)^T\big(\boldsymbol{S}^i_j\big)^{-1}\big(\widetilde{\boldsymbol{\gamma}}^i_j\big)\right]+K, \tag{14}$$

where

$$K=\sum_{j=\theta}^{k}\ln\big|\boldsymbol{S}^0_j\big|-\sum_{i=1}^{n}\omega^i\sum_{j=\theta}^{k}\ln\big|\boldsymbol{S}^i_j\big|$$

is independent of the measurements. According to (14), in order to obtain filter innovations based on n measurement equations, several measurement equations (as many measurement equations as the number of bias magnitude samples) have to be processed in parallel and the contributions of all these measurement equations are weighted by ω^i. In such case, each sample v_i corresponds to one measurement equation, and the weight of each measurement equation actually depends on how close the magnitude sample v_i is to the exact magnitude v. Thus, the weight associated with each measurement equation is time-varying (hidden Markov chain) which will be denoted as $\widetilde{\omega}^i_j$ (weight of the i-th measurement equation at time j). After replacing ω^i by $\widetilde{\omega}^i_j$ in (14), the following result can be obtained

$$\tilde{l}_k(\theta)=\sum_{j=\theta}^{k}\left[\big(\boldsymbol{\gamma}^0_j\big)^T\big(\boldsymbol{S}^0_j\big)^{-1}\big(\boldsymbol{\gamma}^0_j\big)-\sum_{i=1}^{n}\widetilde{\omega}^i_j\big(\widetilde{\boldsymbol{\gamma}}^i_j\big)^T\big(\boldsymbol{S}^i_j\big)^{-1}\big(\widetilde{\boldsymbol{\gamma}}^i_j\big)\right]+K', \tag{15}$$

where

$$K'=\sum_{j=\theta}^{k}\left[\ln\big|\boldsymbol{S}^0_j\big|-\sum_{i=1}^{n}\widetilde{\omega}^i_j\ln\big|\boldsymbol{S}^i_j\big|\right].$$

Finally, using the previous derivations, the presence of a mean value jump is accepted or rejected using the following rule

$$\tilde{l}_k(\hat{\theta})\underset{\mathrm{H}_0}{\overset{\mathrm{H}_1}{\gtrless}}\varepsilon',$$

where ε' is a threshold related to the probability of false alarm of the test, and $\hat{\theta}$ is the MLE of the occurrence time θ. Thus $\hat{\theta}$ can be defined as

$$\hat{\theta}=\underset{\theta}{\operatorname{argmax}}\,\tilde{l}_k(\theta).$$

The rest of this section discusses the way of adjusting the weights $\widetilde{\omega}_j^i$ defining $\tilde{l}_k(\theta)$. Considering that several measurement equations need to be processed in parallel, $\widetilde{\omega}_j^i$ can be computed based on the IMM algorithm [18]. A set of measurement models associated with the jump magnitude samples v_i $(i = 1, \dots, n)$ is denoted as

$$M \triangleq^{\text{def}} \{M^i\}_{i=1}^n,$$

and the corresponding model probability $\widetilde{\omega}_j^i$ can be obtained based on the current measurement $\boldsymbol{Z}_j$ and the predicted model probability, leading to

$$\begin{aligned}\widetilde{\omega}_j^i &= p\left(M_j^i \middle| \boldsymbol{Z}_j\right) \\ &= \frac{1}{c} p\left(\widetilde{\boldsymbol{\gamma}}_j^i \middle| \mathrm{H}_1(\theta, v_i)\right) p\left(M_j^i \middle| \boldsymbol{Z}_{j-1}\right),\end{aligned}$$

where $j = \theta, \dots, k$ and c is the normalization constant.

IV. IDENTIFICATION/ESTIMATION/CORRECTION OF NLOS MP BIASES

According to the test statistic $\tilde{l}_k(\theta)$ resulting from the approximate MLRT derived in section III, the occurrence time of the NLOS MP bias can be estimated. In order to determine which pseudo-range measurements are affected by NLOS MP bias, we study in this section a simultaneous detection and identification procedure. Note that the pseudo-range measurements associated with a mean value jump are usually isolated after the presence of an MP interference has been confirmed by standard integrity checks, such as the Receiver Autonomous Integrity Monitoring (RAIM) method [1]. However, considering that the number of in-view satellites is limited in urban scenarios, the exclusion of pseudo-range measurements may weaken the observability and impair the accuracy of positioning solution based on GNSS. In order to implement the positioning solution with a maximum of pseudo-range measurements, we propose in this paper to estimate the NLOS MP biases and to correct this presence of bias in the measurements. All these operations referred to as identification, estimation and correction are detailed below.

A. Identification of NLOS MP Biases

In order to make identification possible, a possible method is to compute one MLRT test statistic for each in-view satellite pseudo-range measurement. In this case, two hypotheses for detecting the presence of NLOS MP bias on the τ-th ($\tau = 1, \dots, N_s$) in-view satellite pseudo-range measurement can be defined as follows

H_0^τ: no mean value jump for the τ-th measurement up to present time k

H_1^τ: a mean value jump (of amplitude $v^\tau \neq 0$) has occurred for the τ-th measurement at time $\theta < k$

The detection and identification of NLOS MP biases can be converted into a group of hypothesis tests for all pseudo-range measurements. The corresponding test statistic $\tilde{l}_k^\tau(\theta)$ $(\tau = 1, \dots, N_s)$ associated with the hypothesis of an NLOS MP bias affecting the τ-th in-view satellite pseudo-range measurement from time θ to k, can be obtained based on the approximate MLRT theory presented in Section III. The MLE of the occurrence time θ associated with the τ-th measurement is

$$\hat{\theta}^\tau = \underset{\theta}{\operatorname{argmax}}\, \tilde{l}_k^\tau(\theta).$$

For detecting the presence of an NLOS MP bias at a possible occurrence time $\hat{\theta}^\tau$, the decision rule can be defined as

$$\tilde{l}_k^\tau\left(\hat{\theta}^\tau\right) \underset{\mathrm{H}_0^\tau}{\overset{\mathrm{H}_1^\tau}{\gtrless}} \varepsilon',$$

where ε' is the τ-th hypothesis threshold related to a given probability of false alarm. In order to simplify the computation, a set of possible amplitudes (for the NLOS MP biases) v_i $(i = 1, \dots, n)$ can be uniformly sampled in the interval (v_{min}, v_{max}), and used for each calculation of the test statistic $\tilde{l}_k^\tau(\theta)$. Finally, it is important for the simultaneous detection and identification to ensure that the proposed approximate MLRT can handle several NLOS MP biases occurring at the same time instant.

B. Estimation and Correction of NLOS MP Biases

The optimization of $\hat{\theta}$ is constrained to the data belonging to a finite window $(k - L_w < \hat{\theta} \leq k)$. In order to reduce the influence of false alarms, the NLOS MP bias in the presence of the τ-th pseudo-range measurement will be confirmed when $\hat{\theta}_k^\tau = k - L_w + 1$. Thus the choice of L_w results from a tradeoff between fast bias detection and accurate bias estimation. Since the bias detection has to be performed in real time, the value of L_w is set to a relatively small value, i.e., $L_w = 5$ in [13] or $L_w = 11$ in [14]. Note that a larger threshold could be chosen to control the false alarm probability.

After it is confirmed that the τ-th satellite pseudo-range measurement has been affected by the NLOS MP interference, we propose to estimate the magnitude of the NLOS MP bias. Since the IMM algorithm is used to update the measurement model probabilities associated with the magnitude samples used in the proposed approximate MLRT, the model probability $\widetilde{\omega}_j^i$ depends on how close the magnitude sample v_i is to the exact magnitude v and can adaptively adjust for each magnitude sample v_i $(i = 1, \dots, n)$. The bias magnitude estimation $\hat{v}^\tau\left(\hat{\theta}_k^\tau\right)$ for the τ-th in-view satellite pseudo-range measurement can be defined as

$$\hat{v}^\tau\left(\hat{\theta}_k^\tau\right) = v_{\hat{\imath}_k} + \hat{r}_{\hat{\imath}_k}^\tau\left(\hat{\theta}_k^\tau\right), \tag{16}$$

with

$$\hat{\imath}_k = \underset{i}{\operatorname{argmax}}\, \widetilde{\omega}_k^i$$

and

$$\hat{r}_{\hat{\imath}_k}^\tau\left(\hat{\theta}_k^\tau\right) = \frac{1}{L_w} \sum_{j=\hat{\theta}_k^\tau}^{k} \tilde{\gamma}_{\hat{\imath}_k,j}^\tau,$$

where

- n is the number of bias magnitude samples,
- $v_{\hat{\imath}_k}$ is the $\hat{\imath}_k$-th sampling value of NLOS multipath bias magnitude,
- $\tilde{\gamma}_{\hat{\imath}_k,j}^\tau = Z_j^\tau - \hat{Z}_{\hat{\imath}_k,j/j-1}^\tau$ is the filter innovation under

hypothesis H_1^τ with bias sampling magnitude v_{i_k},

- Z_j^τ and $\hat{Z}_{i_k,j/j-1}^\tau$ are the τ-th in-view satellite pseudo-range and predicted pseudo-range measurements under hypothesis H_1^τ with a jump magnitude v_{i_k} at time j, respectively.

Once the NLOS MP bias and its magnitude have been confirmed and estimated, we propose to correct the corresponding filter innovation and to use it for the positioning solution based on the standard EKF algorithm. For the τ-th pseudo-range measurement which is affected by the NLOS MP bias, the corresponding filter innovation can be corrected as follows

$$\bar{\gamma}_k^\tau = \gamma_k^\tau - \hat{v}^\tau(\hat{\theta}_k^\tau), \tag{17}$$

where

- $k = \hat{\theta}_k^\tau + L_w - 1$,
- $\bar{\gamma}_k^\tau$ is the corrected filter innovation which will be used in EKF algorithm at time k,
- $\gamma_k^\tau = Z_k^\tau - \hat{Z}_{k/k-1}^\tau$ is the filter innovation under hypothesis H_0^τ at time k,
- $\hat{Z}_{k/k-1}^\tau$ is the predicted pseudo-range measurement of the τ-th in-view satellite under hypothesis H_0^τ at time k.

Note that the objective of correcting the filter innovation rather than the pseudo-range measurement is to enable the detection of NLOS MP bias during its whole duration.

V. SIMULATION RESULTS

Several simulations have been implemented to validate the proposed approximate MLRT approach. The state space model has been simulated with the parameters reported in Tab. I. The fault-free GNSS measurements have been computed based on an almanac file including all useful satellite orbit data. In theory, the pseudo-range MP error can reach magnitudes close to 0.5 of a code chip [10], i.e., 150m in the C/A case, depending on the receiver correlation technology; We have assumed that the prior distribution of the MP bias magnitude v is a uniform distribution in the interval [-75, 75], i.e., $p(v)$~U(-75, 75). Due to the excessive competition between unnecessary models, the performance of the IMM algorithm decreases when too many models are considered. The number of bias magnitude samples used in our simulations has been set to $n = 5$.

TABLE I. SIMULATION PARAMETERS

Process noise (velocity)	$\sigma_a = 1\,\mathrm{m/s^{-2}}$
Clock offset noise [a]	$\sigma_b = 4\pi c \times 10^{-9}\mathrm{m}$
Clock drift noise [a]	$\sigma_b = 2c \times 10^{-10}\mathrm{m}$
GNSS measurement noise	$\sigma_r = 10\mathrm{m}$

[a] $c = 3 \times 10^8\mathrm{m/s}$ denotes the velocity of light

According to the hypothesis testing theory, the rejected region associated with absence of NLOS MP bias needs to be determined based on the distribution function of test statistic under hypothesis H_0 and significance level α (false alarm rate). Based on the aforementioned derivations, the expression of the test statistic $\tilde{l}^\tau(\theta)$ in the proposed approximate MLRT under hypothesis H_0^τ has not a closed-form expression and thus the explicit distribution function of the test statistic $\tilde{l}^\tau(\theta)$ under hypothesis H_0^τ cannot be determined. Therefore, the empirical cumulative distribution function (cdf) of the test statistic $\tilde{l}^\tau(\theta)$ under hypothesis H_0^τ has been computed using MC simulations performed using an appropriate GNSS pseudo-range measurement noise. Based on the above simulation parameters, the cdfs associated with different data window lengths for one satellite pseudo-range measurement are depicted in Fig. 1. The thresholds corresponding to different false alarm ratios are presented in Tab. II. In order to reduce the influence of false alarms, the threshold has been set to ensure a false alarm rate of 0.05. It is assumed that there are 4 in-view satellite pseudo-range measurements and that the NLOS MP biases affecting the satellite pseudo-range measurements have been generated according to the measurement model (2) as follows

- The first satellite pseudo-range measurement (satellite #1) is affected by a mean value jump of 40m during the time interval [40s, 70s], and an NLOS MP bias of -40m appears during the time interval [120s, 140s],
- The second satellite pseudo-range measurement (satellite #2) is affected by an NLOS MP bias of 55m occurring during the time interval [100s, 150s].

Finally the length of the data window is $L_w = 4$ and the filter period equals 1Hz in all simulations. We propose to compare the positioning and bias magnitude estimation accuracy of the proposed bias detection/estimation approach with those obtained using a standard EKF. M = 50 MC simulations have been run to compute the estimation mean value and root mean square errors (RMSE) denoted by $M^{-1}\sum_{i=1}^{M}\hat{\boldsymbol{X}}_k^{(i)}$ and $\sqrt{M^{-1}\sum_{i=1}^{M}\left(\hat{\boldsymbol{X}}_k^{(i)} - \boldsymbol{X}_k\right)^2}$, where $\hat{\boldsymbol{X}}_k^{(i)}$ is the i-th run result, and $k = 1, \ldots, \infty$ denotes the sampling time instant.

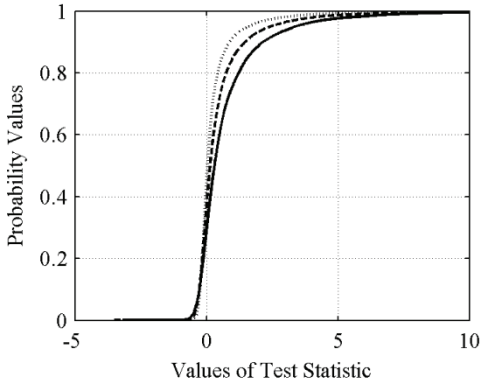

Figure 1. Empirical cdf associated with different data window lengths. L_w = 4 (dotted line). $L_w = 7$ (dashed line). $L_w = 11$ (solid line).

TABLE II. THRESHOLDS FOR DIFFERENT FALSE ALARM RATIOS

Length of Data Window L_w	**False Alarm Rate α**		
	0.025	***0.05***	***0.1***
4	2.531	1.602	0.880
7	3.628	2.431	1.472
11	4.811	3.402	2.163

Fig. 2 shows the magnitude estimations of NLOS MP biases for pseudo-range measurements #1 and #2 versus simulation time. The corresponding bias RMSEs are depicted in Fig. 3. Since the prior information about the bias magnitude

is taken into account, the proposed approach can track the biases with good accuracy. Note that a switching between the different measurement models is considered in the IMM algorithm. Thus, when the NLOS MP bias occurs, peak errors due to bias estimation can be clearly observed. After the measurement model has been determined, the bias estimations become stable and the bias RMSEs decrease to less than 10m in the presence of a mean value jump. In addition, there are some false alarms leading to bias estimation errors in the absence of mean value jump as shown in Fig. 3.

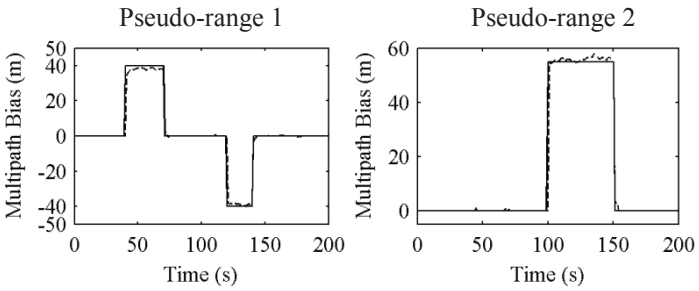

Figure 2. Magnitude estimated of NLOS MP biases for the pseudo-range measurements #1 and #2 (50 MC runs). Actual bias magnitude (solid line). Estimated bias magnitude (dashed line).

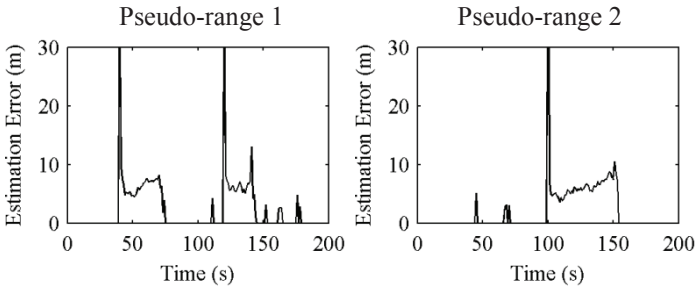

Figure 3. RMSEs of bias magnitudes (50 MC runs).

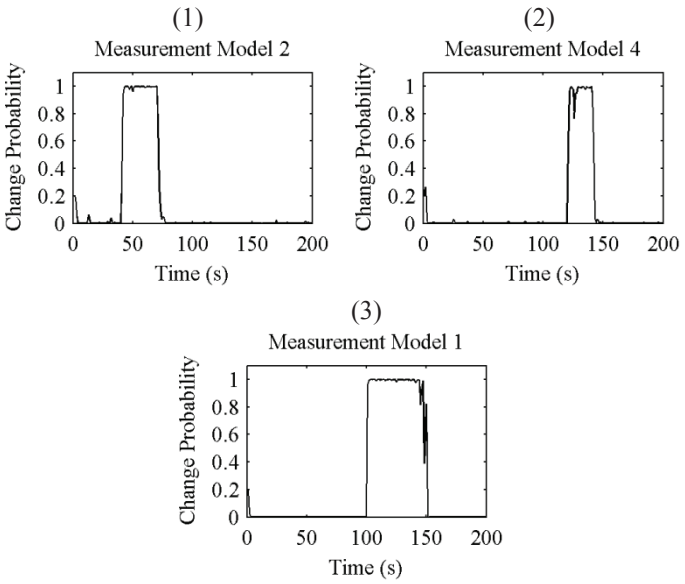

Figure 4. Change probabilities of different models versus simulation time provided by the IMM algorithm. (1) Bias magnitude v_2 = 30.36m for model #2 (2) Bias magnitude v_4 = -45.83m for model #4. (3) Bias magnitude v_1 = 65.98m for model #1.

Fig. 4 shows the change probabilities of the different models used for the pseudo-range measurements #1 and #2 in the IMM algorithm (a high probability indicates a very likely presence of a mean value jump whereas a small probability corresponds to a measurement non affected by NLOS MP). It is clear that the corresponding change of model probability is in good agreement with the occurrence of the NLOS MP bias. The advantage of using the IMM algorithm is to adaptively update the prior information about the bias magnitude based on the filter innovation.

The RMSEs of the positioning estimations based on the standard EKF in three directions are depicted in Fig. 5. The positioning accuracy obtained with the standard EKF is reduced because the MP biases are not mitigated. Conversely, the positioning accuracy significantly improves when using the proposed approach. Since the estimation of the bias magnitude is affected by some error, the positioning accuracy in the presence of NLOS MP bias is smaller than that obtained in absence of NLOS MP bias.

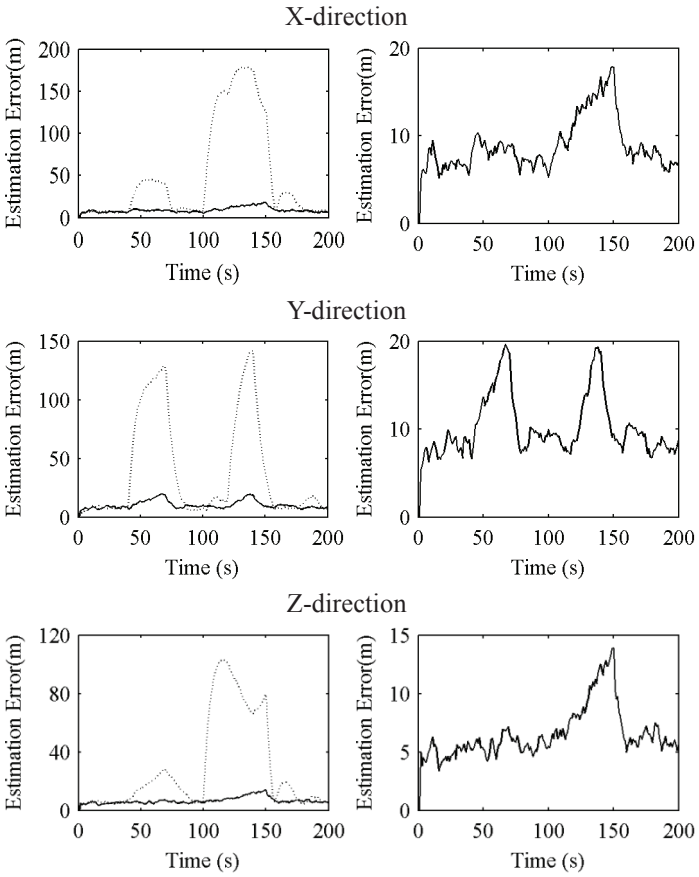

Figure 5. RMSEs of positioning estimations in three directions (50 MC runs). The proposed approach (soild line). The standard EKF (dotted line).

VI. CONCLUSION

This paper proposed an approximate marginalized likelihood ratio test based on Jensen's inequality to detect, identify and estimate the non-line-of-sight multipath biases affecting GNSS pseudo-range measurements in urban canyons. Moreover, the interacting multiple model algorithm was introduced to update the prior information of each bias magnitude sample to improve its estimation. The theoretical

results were validated by simulations, showing the interest of the proposed approach.

The number of bias magnitude samples used in the algorithm can be large in some cases to ensure an accurate Monte Carlo integration. Moreover, the performance of the IMM algorithm can decrease when too many models are considered (it is due to the excessive competition between unnecessary models). Future work will be devoted to the study of as variable structure multiple model as the one developed in [19] which might bypass these difficulties.

ACKNOWLEDGMENT

This work was supported by the National Natural Science Foundation of China (Project #61135001, #61075029).

REFERENCES

[1] P. D. Groves, *Principles of GNSS, Inertial and Multisensor Integrated Navigation Systems*, Boston, MA: Artech House, 2008.

[2] Z. Y. Jiang and P. D. Groves. "NLOS GPS signal detection using a dual-polarisation antenna," *GPS Solutions*, vol. 18, no. 1, pp. 15-26, January 2014.

[3] S. Daneshmand, A. Broumandan, N. Sokhandan, and G. Lachapelle, "GNSS multipath mitigation with a moving antenna array," *IEEE Trans. on Aerospace and Electronic Systems*, vol. 49, no. 1, pp. 693-698, January 2013.

[4] N. Jardak, A. Vervisch-Picois, and N. Samama, "Multipath insensitive delay lock loop in GNSS receivers," *IEEE Trans. on Aerospace and Electronic Systems*, vol, 47, no. 4, pp. 2590-2609, October 2011

[5] N. Blanco-Delgado and F. D. Nunes, "Multipath estimation in multicorrelator GNSS receivers using the maximum likelihood principle," *IEEE Trans. on Aerospace and Electronic Systems*, vol. 48, no. 4, pp. 3222-3233, October 2012

[6] S. F. Syed Dardin, V. Calmettes, B. Priot, and J.-Y. Tourneret, "Design of an adaptive vector-tracking loop for reliable positioning in harsh environment," in *Proc. of ION GNSS 2013*, Nashville, Tennessee, September 22-25, 2013.

[7] P. D. Groves, "Shadow Matching: A new GNSS positioning technique for urban canyons", *J. of the Institute of Navigation*, vol. 64, pp. 417–430, July 2011.

[8] D. E. Gustafson, J. Elwell, and J. Soltz, "Innovative indoor geolocation using RF multipath diversity," in *Proc. of IEEE/ION PLAN 2006*, San Diego, California, April 25-27, 2006.

[9] A. Bourdeau, M. Sahmoudi, and J.-Y. Tourneret. "Constructive use of GNSS NLOS-multipath: Augmenting the navigation Kalman filter with a 3D model of the environment," in *Proc. of IEEE International Conference on Information Fusion 2012*, Singapore, July 9-12, 2012.

[10] E. Kaplan, *Understanding GPS: Principles and Applications 2nd Edition*, Boston, MA: Artech House, 2006.

[11] M. Spangenberg, V. Calmettes, O. Julien, J.-Y. Tourneret, and G. Duchateau, "Detection of variance changes and mean value jumps in measurement noise for multipath mitigation in urban navigation," *J. of the Institute of Navigation*, vol. 57, no. 1, pp. 35-52, Spring 2010.

[12] N. Viandier, D. Nahimana, J. Marais, and E. Duflos, "GNSS performance enhancement in urban environment based on pseudo-range error model," in *Proc. of IEEE/ION PLAN 2008*, Monterey, California, May 5-8, 2008.

[13] A. Giremus, J.-Y. Tourneret, and V. Calmettes, "A particle filtering approach for joint detection/estimation of multipath effects on GPS measurements," *IEEE Trans. Signal Process*, Vol. 55, No. 4, pp. 1275-1285, April 2007

[14] A. S. Willsky and H. L. Jones, "A generalized likelihood ratio approach to the detection and estimation of jumps in linear systems," *IEEE Trans. Automatic Control*, vol. 21, no. 1, pp. 108-112, February 1976.

[15] F. Gustafsson, "The marginalized likelihood ratio test for detecting abrupt changes," *IEEE Trans. Automatic Control*, vol. 41, no. 1, pp. 66-78, January 1996.

[16] A. Giremus and J. Grolleau, "An unscented Kalman filter based maximum likelihood ratio for NLOS bias detection in UMTS localization," in *Proc. of Eur. Signal Processing Conference*, Lausanne, Switzerland, August 25-29, 2008.

[17] D. J. C. MacKay, *Information Theory, Inference and Learning Algorithms*, Cambridge: Cambridge University Press, 2003.

[18] Y. Bar-Shalom, X. R. Li, and T. Kirubarajan, *Estimation with Applications to Tracking and Navigation: Theory Algorithms and Software*, New York: John Wiley & Sons, 2001.

[19] J. Lan, X. R. Li, and C. D. Mu, "Best model augmentation for variable-structure multiple-model estimation," *IEEE Trans. on Aerospace and Electronic System,* vol 47, no. 3, pp. 2008-2025, July 2011.